

RESEARCH ARTICLE

10.1002/2015JA021993

Neutron monitor yield function for solar neutrons: A new computation

A. A. Artamonov¹, G. A. Kovaltsov², A. L. Mishev³, and I. G. Usoskin^{1,3}¹Sodankylä Geophysical Observatory (Oulu unit), University of Oulu, Oulu, Finland, ²Ioffe Physical-Technical Institute of Russian Academy of Sciences, St. Petersburg, Russia, ³ReSolVE Center of Excellence, University of Oulu, Oulu, Finland

Key Points:

- A new neutron monitor yield function for solar neutrons is presented
- The ability of the neutron monitor network to detect a solar neutron event is studied
- It is shown that the NM network is a useful tool to study solar neutron events

Correspondence to:

I. G. Usoskin,
ilya.usoskin@oulu.fi

Citation:

Artamonov, A. A., G. A. Kovaltsov, A. L. Mishev, and I. G. Usoskin (2016), Neutron monitor yield function for solar neutrons: A new computation, *J. Geophys. Res. Space Physics*, 121, 117–128, doi:10.1002/2015JA021993.

Received 6 OCT 2015

Accepted 7 JAN 2016

Accepted article online 13 JAN 2016

Published online 30 JAN 2016

Abstract A new yield function of a standard neutron monitor 6NM64 for solar neutrons is presented and tabulated in the attached lookup tables. It corresponds to a wide range of altitudes of the neutron monitor locations and angles of incidence for neutrons entering the Earth's atmosphere. The computations were made by Monte Carlo using the GEANT4-based PLANETOCOSMICS tool. The yield function was validated against the measured data for solar neutron events of 3 June 1982 and 24 May 1990, and good agreement was found within a wide range of the altitudes of the neutron monitor location and angles of incidence of solar neutron arrival. The sensitivity of the world neutron monitor network for registration of solar neutron events was reassessed. The neutron monitor network is shown to be, in addition to other methods, a sensitive tool for monitoring of high-energy solar-flare neutrons with $\approx 95\%$ probability to detect statistically significantly ($> 5\sigma$) a solar neutron event similar to that of 3 June 1982.

1. Introduction

Occasionally, during eruptive events, such as solar flares, nucleons, mostly protons and α - particles, can be accelerated up to high energies in the solar atmosphere and interact with the matter in nuclear reactions. As a result, neutrons can be produced locally, which may escape into the interplanetary space [e.g., *Chupp*, 1988; *Chupp and Ryan*, 2009; *Dorman*, 2010; *Vilmer et al.*, 2011]. Such neutrons are conventionally called "solar neutrons." Since transport of neutrons is not affected by magnetic fields, they propagate straight from the Sun. Free neutrons are unstable with the mean lifetime of about 887.7 s [*Yue et al.*, 2013], which is comparable to the time of flight of energetic neutrons from Sun to Earth, but if their energy is sufficiently high, a major fraction of the escaped neutrons can survive until reaching the Earth's orbit at 1 AU and can be detected by space-borne detectors. Because of the thick atmosphere, only a very small fraction of the primary particles can penetrate through it. If the energy of a solar neutron exceeds several hundred MeV, the nucleonic cascade in the Earth's atmosphere becomes essential, leading to enhanced flux of secondary nucleons near the ground, similar to cosmic rays. Products of such cascades, initiated by solar neutrons, can be detected, as solar neutron events (SNEs) by the ground-based network of neutron monitors (NMs). It is important that not the primary solar neutrons, but mostly, secondary nucleonic products of the atmospheric cascade are detected by the ground-based NMs. During the past 35 years, 12 such solar neutron events have been detected by the NM network [*Debrunner et al.*, 1983; *Efimov et al.*, 1983; *Chupp et al.*, 1987; *Smart et al.*, 1990; *Pyle and Simpson*, 1991; *Shea et al.*, 1991; *Debrunner et al.*, 1993; *Struminsky et al.*, 1994; *Muraki et al.*, 1995, 2008; *Watanabe et al.*, 2003, 2007; *Bieber et al.*, 2005], with the average rate of several events per solar cycle. However, no strong SNE has been detected during the present solar cycle # 24.

Information on the energy spectrum of solar neutrons complemented by the measurements of the γ -radiation produced in the solar atmosphere during solar flares and by solar energetic particles (SEPs) in the interplanetary space can be useful in studying of acceleration and transport of nucleons with energy above 100 MeV/nucleon in the solar atmosphere [e.g., *Dorman*, 2010, and references therein]. Solar neutrons can be studied indirectly via γ -emission of the 2.223 MeV neutron-capture line [e.g., *Hua and Lingenfelter*, 1987], providing information on neutrons (energy < 20 MeV) interacting in the photosphere, and/or via detection of neutron-decay protons [e.g., *Evenson et al.*, 1990] and electrons [*Dröge et al.*, 1996] produced as a result of decay of escaped solar neutron (energy below 100 MeV) in the interplanetary space. Direct observations of neutrons in space were limited to lower (about 100 MeV) energy [e.g., *Chupp et al.*, 1987; *Kocharov et al.*, 1998; *Kuznetsov et al.*, 2011], but modern space-borne missions Alpha Magnetic Spectrometer-02

[Aguilar *et al.*, 2013] and Payload for Antimatter Matter Exploration and Light-nuclei Astrophysics [Adriani *et al.*, 2014] have full capacity to directly measure solar neutrons. The high-energy tail of the solar neutron population can be also measured on ground by a dedicated network of high-altitude solar neutron telescopes [Matsubara *et al.*, 2005], which are tuned to directly measure solar neutrons, attenuated in the atmosphere, and have sensitivity of about 30% [Valdes-Galicia *et al.*, 2009]. These methods are well developed and lie beyond the scope of this work.

The high-energy solar neutrons were often measured by NMs [Yu *et al.*, 2015], especially in earlier years. The worldwide network of NMs, which was not originally designed for such studies, can provide without any additional investments, useful information on this, complementing other dedicated measurements, such as γ -emission or direct detection of neutrons in space or high altitudes. A new method considering the NM network as a whole instrument was proposed by Usoskin *et al.* [1997] which increases the signal-to-noise ratio for study of SNEs. Here we revisited this method using the new yield function of a NM and reassess the sensitivity of the existing NM network to solar neutrons.

For an analysis of a SNE detected by the NM network one needs to know the yield function of a ground-based NM to primary neutrons impinging on the top of the atmosphere. The yield function is defined as the response of a standard NM to the monoenergetic unit flux of the primary particles entering the Earth's atmosphere with a given angle of incidence. The use of a yield function is a usual way to study the spectral and temporal variabilities of the galactic cosmic rays (GCR) and solar particle events (ground-level enhancements) using the NM network [e.g., Clem and Dorman, 2000; Vashenyuk *et al.*, 2007; Mishev *et al.*, 2013; Caballero-Lopez and Moraal, 2012; Aiensa-ad *et al.*, 2015]. The validity of the yield function and, in particular, the account for energy-dependent effective area of the NM [Mishev *et al.*, 2013] was confirmed by achieving good agreement between model results and measurements [e.g., Gil *et al.*, 2015]. In these cases, the primary particles initiating the atmospheric cascade are protons and α -particles [Mishev *et al.*, 2013], but to study SNEs one needs the NM yield function for primary neutrons. An important difference between solar neutrons and GCR/SEP is the angular distribution of the primary particles. The GCR flux is almost fully isotropic, and SEP flux is either isotropic or with a finite wide angular distribution around the magnetic line connecting Earth to the Sun, because of the scattering on magnetic inhomogeneities along the path in the interplanetary space. Conversely, the solar neutrons arrive as a single-directional beam coming straight from the Sun.

Thus, the relative Sun-Earth geometry is important for the detection of a SNE. Since the atmosphere attenuates the flux of secondary nucleons of the cascade, the response of a NM to SNE is higher when the atmospheric depth in the solar direction is smaller. The most effective is a high-altitude NM measuring the event at the local noon, when the solar zenith angle is the smallest, and a wide network of such NMs is needed so that, when the event occurs, at least some detectors can see the Sun at small zenith angle [Usoskin *et al.*, 1997]. Therefore, a set of NM yield functions for primary neutrons, calculated for a wide range of neutron angles of incidence and different atmospheric depths, is necessary for a proper analysis of the SNEs. Until present, such yield functions were available only for a very limited set of angles of incidence and depths [Chupp *et al.*, 1987; Efimov and Terekhov, 1988; Efimov, 1997; Shibata, 1994; Debrunner *et al.*, 1997]. Moreover, as discussed in Usoskin *et al.* [1997], earlier computations disagree between each other. Accordingly, empirical relations were often in use [e.g., Usoskin *et al.*, 1997; Dorman *et al.*, 1999].

In this work we present a newly computed yield function of a standard NM for solar neutrons in a wide range of the incidence angles and atmospheric depths. The sensitivity of the world NM network as a single instrument to study SNEs is calculated.

2. The Response of a NM to Solar Neutrons

A NM always counts (variable within a solar cycle) galactic cosmic rays impinging on the atmosphere. A SNE would be observed as an excess above the background, related to a solar flare, during local daytime, especially at high-altitude and low-latitude NMs. The time profile of such an excess represents a convolution between the neutron injection time profile and the flight-time and decay distributions, which are related to the energy spectrum of injected neutrons. In combination with information from other types of detectors (γ -detectors and space-borne instruments), it can help disentangling the energy spectrum from the emission time profile.

Since the count rate of a NM is mostly caused by particles of the atmospheric cascade, it is not straightforward to evaluate the physical flux of primary particles, which is particularly necessary when comparing with other types of measurements. One needs the NM yield function, which is presented here, to do that.

2.1. Formalism

The response of a given NM to solar neutrons depends on the geographical location, the flux of solar neutrons at the Earth's orbit, the type and number of NM counters and physical properties of NM station, and the local time of occurrence of the SNE. The time-integrated response of a NM, N_n , during a SNE is defined as

$$N_n = \int \int F_n(E, t) \cdot S_n(E, h, \alpha) \cdot dE \cdot dt \quad (1)$$

where $F_n(E, t)$ is the flux of solar neutrons at the Earth's orbit, E is the solar neutron kinetic energy, $S_n(E, h, \alpha)$ is the yield function of a NM to primary neutrons, h is the altitude (atmospheric depth) of the NM location, α is the solar zenith angle during the SNE. Integration is over the time of the SNE and energy of solar neutrons.

The expected flux of solar neutrons at the Earth's orbit is given by the following expression:

$$F_n(E) = \frac{D(E)}{R_E^2} \cdot P_s(E) \quad (2)$$

where $D(E)$ is the flux of solar neutrons ejected from the Sun toward the Earth with the kinetic energy E , $R_E^2 = 2.24 \cdot 10^{22} \text{ m}^2 / \text{sr}$ is the area of one steradian on a sphere with radius $R_E = 1 \text{ AU}$, $P_s(E)$ is the survival probability of a solar neutron to reach the Earth:

$$P_s(E) = \exp\left(-\frac{R_E}{\tau c \sqrt{\gamma^2 - 1}}\right), \quad (3)$$

where τ is the neutron mean life time, γ is the Lorentz factor, and c is the light speed in vacuum.

The response of a NM to solar neutrons is a function of the solar zenith angle which can be approximated as

$$\cos \alpha = \sin \varphi \cdot \sin (2\pi\eta) \cdot \sin \varepsilon + \cos \varphi \cdot \sqrt{1 - \sin^2 (2\pi\eta) \sin^2 \varepsilon} \cdot \cos \left(\pi \cdot \left(\frac{T}{12} + \frac{\lambda}{180} - 1 \right) \right) \quad (4)$$

where φ and λ are the latitude (varying from -90° to 90°) and longitude (from 0° to 360°) of the NM location, respectively, $\varepsilon = 23.5^\circ$ is the inclination of the equator relative to the ecliptic plane, η is the fraction of the year since the vernal equinox, and T is the time UT in hours (0–24 h). The yield function S_n gives the response of a NM to the monoenergetic unit flux (one neutron per unit area) of solar neutrons at the Earth's orbit.

According to equations (1)–(4), the response of a given NM to solar neutrons is a function of the altitude above the sea level, the zenith angle of the Sun at the time of the SNE occurrence, the NM location, and the energy of solar neutrons.

2.2. Neutron Monitor Yield Function for Solar Neutrons

In order to compute the response (count rate) of a NM to primary particle flux, one needs to know the NM's yield function (for details see, e.g., *Hatton [1971]*, *Clem and Dorman [2000]*, and references therein) described as S_n in equation (1). The NM yield function incorporates the full complexity of the atmospheric cascade development and secondary particle propagation through the Earth's atmosphere as well as the efficiency of the detector itself to register the secondary particles of the atmospheric cascade. The expression for computing the yield function S_n is

$$S_n(E, h, \alpha) = \sum_i \int \int A_i(E', \theta') \Phi_i(E, h, \alpha; \theta', E') dE' d\Omega' \quad (5)$$

where $A_i(E', \theta')$ is the detector's effective area (the geometrical area corrected for the efficiency of the NM to detect particles of type i), Φ_i is the flux, at the detector's location, of the secondary particles of type i (neutrons, protons, muons, and pions) produced in a cascade initiated by the primary neutron with kinetic energy E and the angle of incidence (on the top of the atmosphere) α , E' is kinetic energy of the secondary particle, θ' being the angle of incidence of secondaries, $d\Omega'$ the solid angle over which the secondaries impinge on the detector.

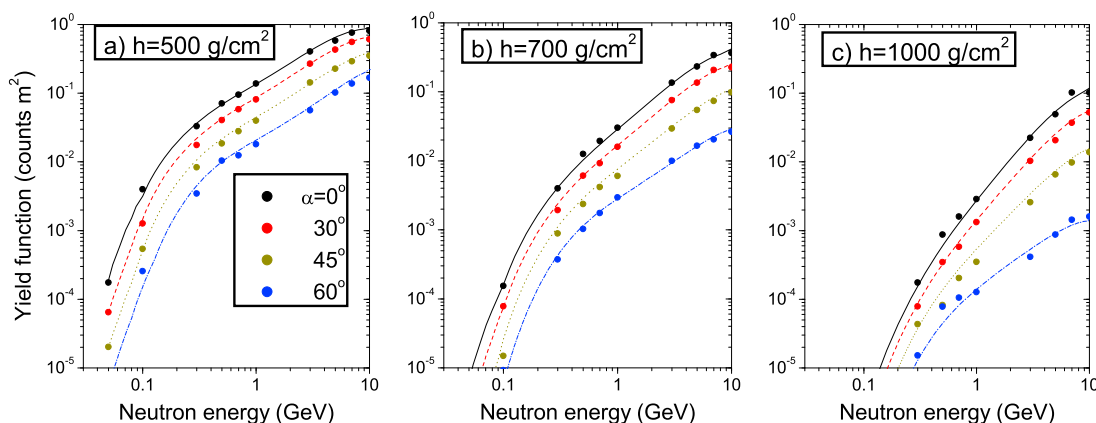


Figure 1. The yield function of a standard 6NM64 neutron monitor to primary solar neutrons (unit flux at the Earth's orbit) with various incidence zenith angles, namely, 0° , 30° , 45° , and 60° at several altitudes: (a) ≈ 5000 m asl (500 g/cm^2); (b) ≈ 3000 m asl (700 g/cm^2); (c) sea level (1000 g/cm^2). The curves are smooth fits of the computed data points. The corresponding lookup tables are given in the appendix.

Here we report a new computation of the yield function of a standard NM (6NM64) for solar neutrons. We use the approach similar to that for the NM yield function for primary protons and α -particles [Mishev *et al.*, 2013]. Full extensive Monte Carlo simulations of the atmospheric cascade caused by energetic neutrons impinging on top of the Earth's atmosphere were performed using the GEANT4 (GEometry ANd Tracking)-based [Agostinelli *et al.*, 2003] PLANETOCOSMICS code [Desorgher *et al.*, 2005] with the use of QGSP_BIC_HP hadron interaction model and the atmospheric model NRLMSISE 2000 [Picone *et al.*, 2002]. We considered energy between 50 MeV and 10 GeV and various incidence angles. The geometrical correction of the yield function due to the finite lateral distribution of the atmospheric cascade, which is important for cosmic ray protons [Mishev *et al.*, 2013], was neglected in this case, because of the relatively low energy range of solar neutrons (the correction plays a role at energies above 10 GeV for vertical incidence, being unlikely for solar neutrons) and features in the cascade development [Debrunner and Brunberg, 1968; Shibata, 1994; Agostinelli *et al.*, 2003; Engel *et al.*, 2011]. This leads to a more conservative estimation (slight underestimation) of the sensitivity of the world NM network for registration of solar neutron events.

Using the Monte Carlo simulations, we calculated fluxes of the secondary particles at the fixed atmospheric level and then convoluted them with the registration efficiency (equation (5)). We used an updated version (J. Clem, B. Gvozdevsky, and E. Mauricev, private communication, 2011–2012) of the NM registration efficiency, originally introduced by Clem and Dorman [2000], considering neutrons, protons, positive and negative pions, and muons that contribute to the count rate of the device [Clem and Dorman, 2000; Mishev *et al.*, 2013].

The results of the computations are given as lookup tables in the appendix (Tables A1–A3). Figure 1 presents some results of the new computations of the yield function of a standard 6NM64 neutron monitor to primary neutrons for several altitudes (atmospheric depths) of the NM locations: $h = 1000 \text{ g/cm}^2$ (about the mean sea level), 700 g/cm^2 (corresponding to a mountain NM at ≈ 3000 m above sea level, a.s.l., altitude) and 500 g/cm^2 (a high-mountain NM at ≈ 5000 m above the sea level). These levels encompass the majority of NMs locations [Mavromichalaki *et al.*, 2011].

One can see that the expected response of a NM to solar neutrons increases as a function of the altitude above the sea level. It also changes with the angle of incidence so that the response is maximal for neutrons with vertical incidence and quickly declines for larger zenith angles. For example, the yield function for 30° incidence neutrons with energy 500 MeV is by a factor 2.5 smaller than that for vertical incidence neutrons, at the sea level.

A comparison of the new yield function with some earlier calculations [Efimov and Terekhov, 1988; Debrunner *et al.*, 1997; Bieber *et al.*, 2005] for specific NMs and events is shown in Figure 2. One can see that, while the new model is in general agreement with the earlier result, in particular with Debrunner *et al.* [1997] and Bieber *et al.* [2005], it is systematically lower than that by Efimov and Terekhov [1988].

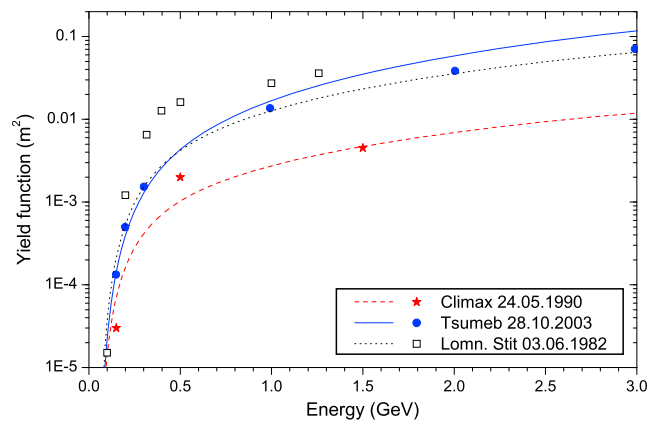


Figure 2. Comparison of the yield function calculated for some specific events and NMs using the present model (lines) with earlier computations (symbols). Red color corresponds to the 12IGY Climax NM during the SNE of 24 May 1990 (stars—computations by *Debrunner et al.* [1997]). Blue color corresponds to the 18NM64 Tsumeb NM during the SNE of 28 October 2003 (dots—computations by *Bieber et al.* [2005]). Black color corresponds to the 8NM64 Lomnický Stit NM during the SNE of 3 June 1982 (squares—computations by *Efimov and M. Terekhov* [1988]).

2.3. Response of a Neutron Monitor to a Solar Neutron Event

Next we evaluated the NM response to a SNE using the approach described above and the newly computed yield function. As the energy spectrum of the solar neutrons ejected from the Sun, we adopted a theoretical spectrum of neutrons produced in the solar matter by energetic nucleons with a power law spectrum (with the proton spectral index 3.5), as calculated by *Hua et al.* [2002, see Figures 7b and 8a therein]. We assumed the isotropic ejection of neutrons from the Sun. We note that the reference SNE spectrum used here is close to that obtained for the event of 3 June 1982 [*Chupp et al.*, 1987, equations (3) and (4)] in the energy range 200 MeV–2 GeV. The corresponding differential energy fluence at the Earth’s orbit is shown as the blue solid line in Figure 3. It was calculated for the reference SNE spectrum corresponding to the total of 10^{33} protons with energy above 30 MeV accelerated in the solar atmosphere. For a comparison, we also show (the red dashed curve) the fluence of injected neutrons, reduced to the Earth’s orbital distance, without considering the neutron decay. One can see that the decay hardens the spectrum. Figures 3b and 3c show the differential response (defined as $F_n \times S_n$, viz., the integrand of equation (1)) of the standard 6NM64 to a SNE for different heights of the NM location and different solar zenith angles at the time of the SNE.

The energy range for effective registration of solar neutrons by NMs (80% of the integral in equation (1)) is between 200–400 MeV and 2–5 GeV, depending on the zenith angle and the altitude. NMs located at higher altitude are more sensitive to lower-energy part of solar neutrons, because of the reduced atmospheric attenuation. In addition, low-latitude NMs possess higher signal-to-noise ratio, because of the high geomagnetic cutoff reducing the GCR background. Therefore, the optimum location of a NM for solar neutron detection is a high mountain at low-middle latitude where the solar zenith angle may be small (see section 3).

2.4. Validation of the Computed NM Response

In order to verify the computations of the new yield function, we have compared the real responses of different NMs with those computed using the new yield function, for two strong SNEs of 3 June 1982 and 24 May 1990, detected by many NMs located at different atmospheric depths and seeing the Sun in a wide range of solar zenith angles. First, we calculated the expected responses of the NM using the method described in section 2.1 and applying the reference neutron fluence, as shown in Figure 3a, keeping its functional form and only scaling it. Accordingly, this is not an analysis of the event but only an indirect validation of the method.

The SNE of 3 June 1982 occurred at about 12 UT and was observed mostly by the European and South African NMs. The highest response was detected by the Lomnický Stit NM located at the atmospheric depth of 765 g/cm² and saw the Sun at the zenith angle of 30.6°. Other NMs considered here are Jungfrauoch IGY ($h = 677$ g/cm², $\alpha = 24.9^\circ$), Rome ($h = 1033$ g/cm², $\alpha = 21.6^\circ$), Kiel ($h = 1033$ g/cm², $\alpha = 33.2^\circ$), Tsumeb ($h = 903$ g/cm², $\alpha = 43.8^\circ$), and Alma-Ata B ($h = 680$ g/cm², $\alpha = 63.6^\circ$). The 6IGY-type neutron monitor is considered as a 0.07 fraction of the 6NM64 one [*Usoskin et al.*, 1997]. Here we compared the actual 5 min peak

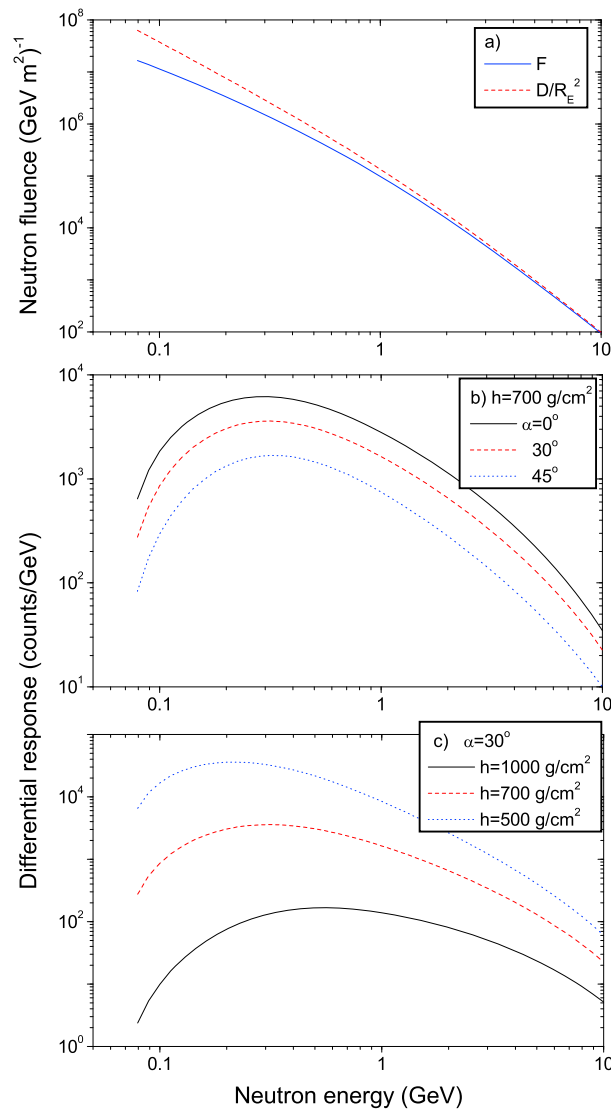


Figure 3. (a) Differential energy fluence of solar neutrons at the Earth orbit. The red dashed line is the fluence without neutron decay taken into account. The calculated fluence F (blue solid line) of solar neutrons at the Earth's orbit. (b) The differential response function of a 6NM64 at 3000 m asl for different zenith angles, 0° , 30° , and 45° , as denoted in the legend; (c) The differential response function of a 6NM64 for the 30° incidence (zenith angle) of solar neutrons for several altitudes: $1000 \text{ g}\cdot\text{cm}^{-2}$ (near-ground level), $700 \text{ g}\cdot\text{cm}^{-2}$ (about 3000 m a.s.l.) and $500 \text{ g}\cdot\text{cm}^{-2}$ (about 5000 a.s.l.), as denoted in the legend.

(11:45–11:50 UT) count rates (data from Table 1 of *Chupp et al. [1987]*, *Stoker [1987]*, and *Zusmanovich and Shwartsman [1987]*) with the model predictions for these angles and depths as shown in Figure 4. The best fit scaling factor for the reference SNE spectrum was found to be 1.1, implying that the reference spectrum is close to that estimated earlier for the SNE of 3 June 1982.

The SNE of 24 May 1990 took place around 21 UT and was detected mostly by North American NMs. The highest response was by the Mexico NM ($h = 790 \text{ g}\cdot\text{cm}^{-2}$, $\alpha = 32.5^\circ$); other considered NMs were Calgary ($h = 895 \text{ g}\cdot\text{cm}^{-2}$, $\alpha = 34.2^\circ$), Inuvik ($h = 1023 \text{ g}\cdot\text{cm}^{-2}$, $\alpha = 47.8^\circ$), Deep River ($h = 1020 \text{ g}\cdot\text{cm}^{-2}$, $\alpha = 52.1^\circ$), Durham ($h = 1029 \text{ g}\cdot\text{cm}^{-2}$, $\alpha = 56.6^\circ$), Climax ($h = 680 \text{ g}\cdot\text{cm}^{-2}$, $\alpha = 30.2^\circ$), Mt. Washington ($h = 820 \text{ g}\cdot\text{cm}^{-2}$, $\alpha = 56.3^\circ$), Newark ($h = 1030 \text{ g}\cdot\text{cm}^{-2}$, $\alpha = 52.7^\circ$), Goose Bay ($h = 1027 \text{ g}\cdot\text{cm}^{-2}$, $\alpha = 63.8^\circ$), and Magadan ($h = 988 \text{ g}\cdot\text{cm}^{-2}$, $\alpha = 65^\circ$). The 5 min (20:50–20:55 UT) peak count rates were taken from Table 1 of *Usoskin*

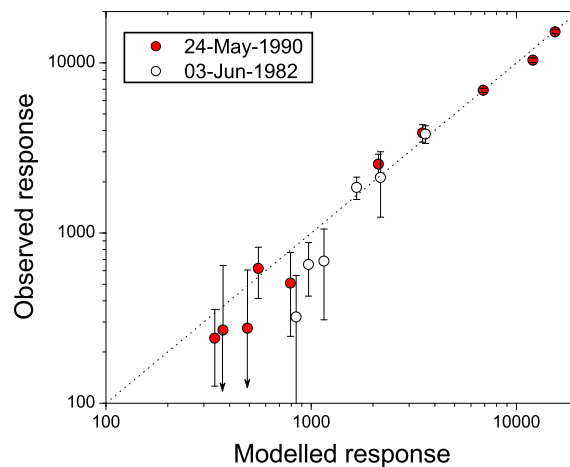


Figure 4. The comparison between the calculations and measurements (dots with error bars) of solar neutron responses (5 min counts with the GCR background removed) for the events of 3 June 1982 and 24 May 1990.

et al. [1997]. The comparison of the modeled and measured peak responses is shown in Figure 4 for the scaling factor to the reference spectrum being 8.

One can see that, despite a wide range of the atmospheric depths (from 680 to 1030 g/cm²) and zenith angles (from 22° to 65°), the agreement between the model and the data is good within the uncertainties. This implies that the model and the new yield function works well for different depths of NM locations and angles of incidence of the solar neutrons.

We note that we do not pretend to make a full analysis of the SNEs [cf. *Chupp et al.*, 1987; *Kocharov et al.*, 1994, 1996; *Debrunner et al.*, 1997] but only test the validity of the new yield function.

3. Sensitivity of the NM Network to a Solar Neutron Event

By using the new yield function, we have estimated, in a way similar to *Usoskin et al.* [1997], the sensitivity of the worldwide NM network to a potential SNE depending on the time it may occur. As the reference event we took the one with the spectrum as in Figure 3a corresponding to the reference spectrum (section 2.3) which is comparable to the event of 3 June 1982. This aims solely for the purpose of illustration of the abilities of the NM network.

We considered the existing NMs with optimal or suitable locations to observe a SNE. The NMs are listed in Table 1 along with their parameters (location, type, geomagnetic rigidity cutoff, and the UT time of the local noon). Figure 5 shows the geographical distribution of NMs from Table 1. For each NM we have computed its expected response to the event depending on the time (day of the year and time UT) of the event occurrence as it defines the solar zenith angle (and thus the angle of incidence for the neutrons), see equation (4). The eccentricity of the Earth's orbit was not taken into account. The response of each NM was quantified in signal-to-noise ratio N/σ , where N is the 5 min count rate (above the background) due to the solar neutrons, and $\sigma = \sqrt{2N_{\text{GCR}}}$ is the statistical noise (the factor 2 appears because of the multiplicity of the NM count rate [Belov *et al.*, 1987]) due to the GCR background count rate. Thus, it quantifies the ability of a NM to detect, with high statistical significance, the SNE above the GCR background. The highest possible response of each NM (if the SNE occurred when the solar zenith angle was minimum possible for a given location) is also listed in Table 1.

An example of the sensitivity of individual NMs to the reference SNE is shown in Figure 6a for two NMs of Tsumeb (South Africa) and Mexico City (Mexico). They are 18NM64 instruments located nearly 120° apart at moderate height in tropical regions. Each of them covers, with good sensitivity, several hours of day time and several months of the year, thus covering ~6% of the time. The two NMs far apart complement each other, and they together cover ~12% of the time with high sensitivity.

Table 1. The List of High-Mountain Neutron Monitors Used Here Along With Their Geographical Coordinates (Latitude and Longitude), Geomagnetic Rigidity Cutoff P_c , Altitudes of NMs Above the Sea Level, Type of NM, UT Time of Local Noon T_{noon} , and the Signal-to-Noise Ratio N_n/σ for the Reference SNE (See Text) if It Occurred at the Local Noon During the Local Summer (the Highest Response)

Name	Latitude	Longitude	P_c (GV)	Altitude, (m)	Type	T_{noon} (UT)	N_n/σ , Max
Chacaltaya	-16.31	291.85	13.10	5200	12 NM	16.5	56.7
Tibet	30.11	90.53	13.71	4300	28 NM	6.0	53.3
Haleakala	20.72	203.75	12.91	3030	18 NM	22.4	26.1
Inthanon	18.59	98.49	16.8	2560	18 NM	5.4	23.7
Erevan	40.5	44.17	7.6	3250	18 NM	9.1	22.1
ALMA B	43.25	76.92	6.61	3340	18 NM	6.9	21.1
Mt.Norikura	36.11	137.55	11.36	2770	12 NM	2.8	17.6
Tsumeb	-19.20	17.58	9.15	1240	18 NM	10.8	12.0
Mexico	19.33	260.82	9.53	2274	6 NM	18.6	10.5
Erevan 3	40.5	44.17	7.58	2000	18 NM	9.1	9.7
ESOI	33.3	35.78	10.8	2055	6 NM	9.6	9.3
CaLMa	40.38	3.9	6.07	708	15 NM	11.7	9.0
Jungfrauoch NM	46.55	7.98	4.49	3475	3 NM	11.5	8.2
Lomnický Štit	49.20	20.22	3.84	2634	8 NM	10.7	7.5
Bure	44.63	5.91	5.00	2252	3 NM	11.6	7.4
Irkutsk3	51.29	100.55	3.64	3000	6 NM	5.3	7.1
Tbilisi	41.43	44.48	6.73	510	18 NM	9.0	6.9
Irkutsk2	52.37	100.55	3.64	2000	12 NM	5.3	6.7
Baksan	43.28	42.69	5.6	1700	6 NM	9.2	6.1
Beijing	40.08	116.26	9.56	48	18 NM	4.20	5.9
Jungfrauoch IGY	46.55	7.98	4.49	3475	18 IGY	11.5	5.3
Rome	41.9	12.52	6.32	60	17 NM	11.2	5.1
Santiago	-33.48	289.29	11.0	570	6 NM	16.7	4.7
Hermanus	-34.25	19.13	4.58	26	12 NM	10.7	4.6
Irkutsk1	52.47	104.03	3.64	435	18 NM	5.1	4.1
Athens	37.98	23.78	8.53	260	6 NM	10.4	3.9
Climax	39.37	253.82	2.99	3400	12 IGY	19.1	3.4
Potchefstroom	-26.68	27.10	6.94	1351	12 IGY	10.2	1.5

However, the abilities of the NM network to detect a SNE is greater than just a sum of individual detectors' responses. The network can be considered as a united detector. For that, responses from different NMs to the event can be compiled using the weighted summation as described in *Usoskin et al. [1997]*.

Let N_i and σ_i be the count rate due to SNE and the noise due to the GCR background, respectively, for i^{th} NM from the list (Table 1). Then the total response of the network X and its uncertainty σ_X are defined as

$$X = \frac{1}{P} \sum_i p_i \cdot N_i \quad \sigma_X = 1/\sqrt{P}, \quad (6)$$

where $p_i = 1/\sigma_i^2$ and $P = \sum p_i$. We note that the signal-to-noise ratio X/σ_X as detected by the network is greater than that for any of the individual NM, since information from all the individual detectors is used. The sensitivity of the NM network to the reference SNE as function of time/date of its occurrence is shown in Figure 7b. One can see that almost all the time is well covered by the high detection ability. Overall, the existing NM network can reliably (at the level of 5σ or better) detect a SNE, similar to that of 3 Jun 1982, with 95% probability. This implies that the NM network is a suitable tool for monitoring strong SNE events, complementing other methods. The network is dominated by two NMs very sensitive to solar neutrons because

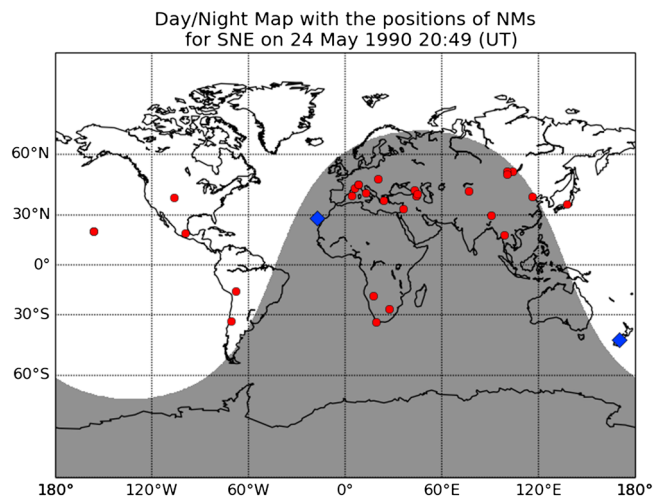


Figure 5. Map of the locations of the NMs considered here (see Table 1). Red circles represent the existing NMs, while the blue diamonds correspond to the proposed new NM stations (Canary islands and New Zealand). The Earth's terminator corresponds to epoch of 24 May 2000, 20:49 UT.

of their location (tropics, high altitude—more than 4000 m a.s.l.) and large size—Chacaltaya and Tibet. They are at least twice more sensitive to solar neutrons than all other NMs in the network. However, just to illustrate the possibilities of the network as a whole, we show (Figure 7a) its sensitivity without these two most sensitive NMs. The region at around 16 UT is not covered in this case since Chacaltaya NM is crucially important for that region, but the removal of the Tibet NM hardly modifies the overall network ability.

One can see that there are two periods when a SNE, if occurred, would remain poorly or not measured. It is a gap at midnight around midwinter, corresponding to the Southern Pacific and a gap in the UT afternoon in the middle of spring-autumn, corresponding to the Atlantic Ocean. Here we propose two new NMs (or solar neutron telescopes) to be located on the Canary Islands and in New Zealand, which might partly cover these gaps. We took as an example locations of the existing facilities of Roque de los Muchachos Observatory (coordinates: 28.76°N 17.89°W, altitude: 2396 m a.s.l.) and Mount John University Observatory (coordinates: 43.59°S 170.29°E, altitude: 1029 m a.s.l.). Figure 6b shows the effect of possible addition of these two NMs (of 12NM64 type) to cover the Atlantic and the Southern Pacific region.

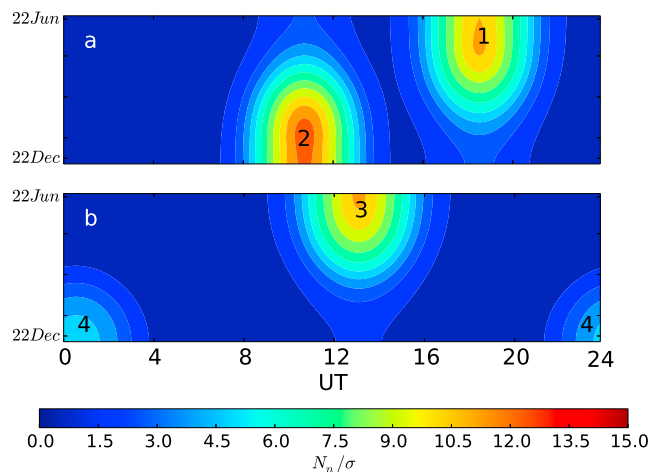


Figure 6. Examples of sensitivity of the individual neutron monitors to the reference SNE as a function of time of occurrence of the event. (a) Mexico NM (1) and Tsumeb NM (2). (b) Possible improvement in world NM network sensitivity with a hypothetical 12NM64 at Canary islands (3) and New Zealand (4).

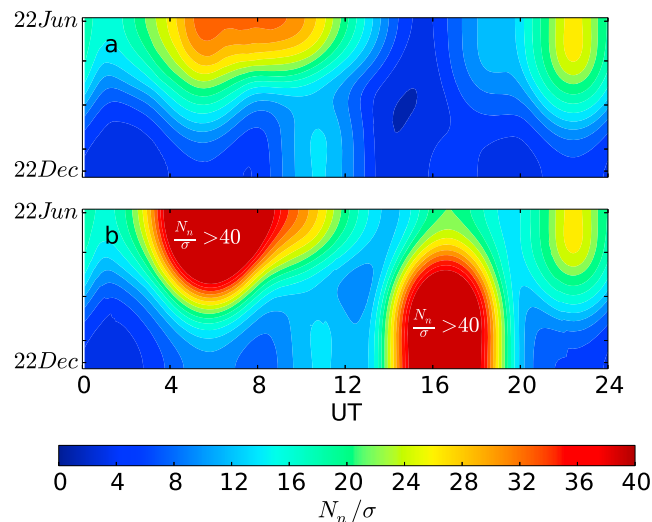


Figure 7. Sensitivity of the world NM network to the reference SNE as function of the time/date of the event occurrence. The sensitivity is calculated for the NM network as a whole, not for individual NMs. (a) The world neutron monitor network without Chacaltaya and Tibet NMs. (b) The world neutron monitor according to Table 1.

4. Conclusions

We have presented a new computations of the yield function of the standard neutron monitor (6NM64) for solar neutrons for a wide range of the altitudes of the NM location and angles of incidence of neutrons entering the Earth’s atmosphere. We provided lookup tables for the newly computed NM yield function for several atmospheric depths of 1000 g/cm² (about the sea level), 700 g/cm² (≈3000 m above the sea level), and 500 g/cm² (≈5000 m above the sea level). The computations were performed using the GEANT4 code PIAN-ETOCOSMICS Monte Carlo tool and a realistic atmospheric model. The yield function was validated against measured data for the solar neutron events of 3 June 1982 and 24 May 1990, and good agreement was found within a wide range of the altitudes of the NM location and angles of incidence of solar neutron arrival. On the basis of the new solar neutron yield function for a standard 6NM64 neutron monitor, the sensitivity of the world NM network for registration of solar neutrons was reassessed. It is shown that NM network is a suitable tool for monitoring of high-energy solar-flare neutrons with good detection efficiency (≈95% probability to detect an event similar to that of 3 June 1982 with a high statistical significance) and complements other techniques to study solar neutrons.

Appendix A: Neutron Monitor Yield Function for Solar Neutrons Lookup Tables

Here lookup tables are presented for the computed neutron monitor (6NM64) yield function for solar neutrons. The tables are for the atmospheric depths of the NM location at 1000 g/cm² (sea level), 700 g/cm² (≈3000 m above the sea level), and 500 g/cm² (≈5000 km above the sea level) and several various angles of incidence. The normalization is for the unit flux (one neutron per square meter) at the Earth’s orbit which is equal to the flux at the top of the atmosphere for the vertical angle of incidence.

Table A1. The Yield Function (in Counts·m⁻²) of a 6NM64 to Solar Neutrons (Unit Flux at the Earth’s orbit), for the Atmospheric Depth of 1000 g/cm² (Sea Level) for Different Incidence Angles

E (GeV)	0°	15°	30°	45°	60°
0.3	1.75 × 10 ⁻⁴	1.54 × 10 ⁻⁴	7.84 × 10 ⁻⁵	4.33 × 10 ⁻⁵	1.52 × 10 ⁻⁵
0.5	8.75 × 10 ⁻⁴	6.15 × 10 ⁻⁴	3.45 × 10 ⁻⁴	8.24 × 10 ⁻⁵	7.81 × 10 ⁻⁵
0.7	1.59 × 10 ⁻³	9.22 × 10 ⁻⁴	5.79 × 10 ⁻⁴	2.03 × 10 ⁻⁴	1.05 × 10 ⁻⁴
1	2.86 × 10 ⁻³	2.15 × 10 ⁻³	1.32 × 10 ⁻³	3.49 × 10 ⁻⁴	1.27 × 10 ⁻⁴
3	2.23 × 10 ⁻²	1.84 × 10 ⁻²	1.03 × 10 ⁻²	2.58 × 10 ⁻³	4.14 × 10 ⁻⁴
5	4.93 × 10 ⁻²	4.46 × 10 ⁻²	2.07 × 10 ⁻²	6.53 × 10 ⁻³	8.75 × 10 ⁻⁴
7	1.02 × 10 ⁻¹	7.38 × 10 ⁻²	3.72 × 10 ⁻²	9.79 × 10 ⁻³	1.43 × 10 ⁻³
10	1.02 × 10 ⁻¹	9.07 × 10 ⁻²	5.24 × 10 ⁻²	1.38 × 10 ⁻²	1.59 × 10 ⁻³

Table A2. The Yield Function (in Counts·m⁻²) of a 6NM64 to Solar Neutrons (Unit Flux at the Earth's Orbit), for the Atmospheric Depth of 700 g/cm² (≈3000 m Above Sea Level) for Different Incidence Angles

E (GeV)	0°	15°	30°	45°	60°
0.05	6.70×10^{-6}	3.63×10^{-6}	2.29×10^{-6}	–	–
0.1	1.54×10^{-4}	1.34×10^{-4}	7.77×10^{-5}	1.49×10^{-5}	9.23×10^{-6}
0.3	3.98×10^{-3}	3.18×10^{-3}	1.93×10^{-3}	8.89×10^{-4}	3.74×10^{-4}
0.5	1.26×10^{-2}	1.05×10^{-2}	6.06×10^{-3}	2.36×10^{-3}	1.03×10^{-3}
0.7	1.93×10^{-2}	1.61×10^{-2}	9.23×10^{-3}	4.16×10^{-3}	1.75×10^{-3}
1	3.01×10^{-2}	2.14×10^{-2}	1.59×10^{-2}	6.03×10^{-3}	2.94×10^{-3}
3	1.35×10^{-1}	1.13×10^{-1}	7.57×10^{-2}	2.93×10^{-2}	9.95×10^{-3}
5	2.32×10^{-1}	2.05×10^{-1}	1.36×10^{-1}	5.47×10^{-2}	1.65×10^{-2}
7	3.41×10^{-1}	2.97×10^{-1}	2.07×10^{-1}	7.36×10^{-2}	2.05×10^{-2}
10	3.66×10^{-1}	3.29×10^{-1}	2.26×10^{-1}	9.84×10^{-2}	2.64×10^{-2}

Table A3. The Yield Function (in Counts·m⁻²) of a 6NM64 to Solar Neutrons (Unit Flux at the Earth's Orbit), for the Atmospheric Depth of 500 g/cm² (≈5000 m Above Sea Level) for Different Incidence Angles

E (GeV)	0°	15°	30°	45°	60°
0.05	1.75×10^{-4}	8.87×10^{-5}	6.46×10^{-5}	2.01×10^{-5}	7.45×10^{-6}
0.1	3.98×10^{-3}	2.15×10^{-3}	1.27×10^{-3}	5.40×10^{-4}	2.55×10^{-4}
0.3	3.31×10^{-2}	2.74×10^{-2}	1.75×10^{-2}	8.33×10^{-3}	3.45×10^{-3}
0.5	7.08×10^{-2}	5.72×10^{-2}	4.05×10^{-2}	1.85×10^{-2}	1.04×10^{-2}
0.7	9.50×10^{-2}	8.82×10^{-2}	5.83×10^{-2}	2.78×10^{-2}	1.24×10^{-2}
1	1.38×10^{-1}	1.18×10^{-1}	8.06×10^{-2}	3.96×10^{-2}	1.81×10^{-2}
3	4.03×10^{-1}	3.55×10^{-1}	2.69×10^{-1}	1.43×10^{-1}	5.62×10^{-2}
5	5.84×10^{-1}	5.37×10^{-1}	4.29×10^{-1}	2.26×10^{-1}	1.02×10^{-1}
7	7.59×10^{-1}	7.03×10^{-1}	5.54×10^{-1}	2.91×10^{-1}	1.38×10^{-1}
10	8.09×10^{-1}	7.72×10^{-1}	6.09×10^{-1}	3.51×10^{-1}	1.67×10^{-1}

Acknowledgments

This work was supported by the Center of Excellence ReSolVE (project No. 272157). We are thankful to J. Clem, B. Gvozdevsky, and E. Mauricev for the updated computation of the NM registration efficiency. Two anonymous reviewers are acknowledged for useful comments. The lookup tables for the new yield functions are available as an appendix to this manuscript.

References

- Adriani, O., et al. (2014), The PAMELA mission: Heralding a new era in precision cosmic ray physics, *Phys. Rep.*, *544*, 323–370, doi:10.1016/j.physrep.2014.06.003.
- Agostinelli, S., J. Allison, and K. Amako (2003), Geant4—A simulation toolkit, *Nucl. Instrum. Methods Phys. Res. Sec. A*, *506*(3), 250–303.
- Aguilar, M., et al. (2013), First result from the alpha magnetic spectrometer on the International Space Station: Precision measurement of the positron fraction in primary cosmic rays of 0.5–350 GeV, *Phys. Rev. Lett.*, *110*(14), 141102, doi:10.1103/PhysRevLett.110.141102.
- Aiemsad, N., et al. (2015), Measurement and simulation of neutron monitor count rate dependence on surrounding structure, *J. Geophys. Res. Space Physics*, *120*, 5253–5265, doi:10.1002/2015JA021249.
- Belov, A. V., L. I. Dorman, V. N. Ishkov, R. A. Saidaliev, and A. G. Zusanovich (1987), Variations of secondary neutrons during powerful solar flares, in *Proceedings of the 20th International Cosmic Ray Conference*, vol. 3, pp. 90–93, Nauka, Moscow.
- Bieber, J. W., J. Clem, P. Evenson, R. Pyle, D. Ruffolo, and A. Sáiz (2005), Relativistic solar neutrons and protons on 28 October 2003, *Geophys. Res. Lett.*, *32*, L03502, doi:10.1029/2004GL021492.
- Caballero-Lopez, R., and H. Moraal (2012), Cosmic-ray yield and response functions in the atmosphere, *J. Geophys. Res.*, *117*, A12103, doi:10.1029/2012JA017794.
- Chupp, E. L. (1988), Solar neutron observations and their relation to solar flare acceleration problems, *Sol. Phys.*, *118*, 137–154, doi:10.1007/BF00148591.
- Chupp, E. L., and J. M. Ryan (2009), High energy neutron and pion-decay gamma-ray emissions from solar flares, *Res. Astron. Astrophys.*, *9*, 11–40, doi:10.1088/1674-4527/9/1/003.
- Chupp, E. L., H. Debrunner, E. Flueckiger, D. J. Forrest, F. Golliez, G. Kanbach, W. T. Vestrand, J. Cooper, and G. Share (1987), Solar neutron emissivity during the large flare on 1982 June 3, *Astrophys. J.*, *318*, 913–925, doi:10.1086/165423.
- Clem, J., and L. Dorman (2000), Neutron monitor response functions, *Space Sci. Rev.*, *93*, 335–359.
- Debrunner, H., and E. Brunberg (1968), Monte Carlo calculation of nucleonic cascade in the atmosphere, *Can. J. Phys.*, *46*, 1069.
- Debrunner, H., E. Flueckiger, E. L. Chupp, and D. J. Forrest (1983), The solar cosmic ray neutron event on June 3, 1982, in *18th Proceedings of International Cosmic Ray Conference*, vol. 4, edited by P. V. Ramana Murthy, pp. 75–78, Tata Institute of Fundamental Research, Bombay, India.
- Debrunner, H., J. A. Lockwood, and J. M. Ryan (1993), Solar neutron and proton production during the 1990 May 24 cosmic-ray flare increases, *Astrophys. J.*, *409*, 822–829, doi:10.1086/172712.
- Debrunner, H., et al. (1997), Energetic neutrons, protons, and gamma rays during the 1990 May 24 solar cosmic-ray event, *Astrophys. J.*, *479*, 997–1011.
- Desorgher, L., E. Flückiger, M. Gurtner, M. Moser, and R. Büttiker (2005), A GEANT 4 code for computing the interaction of cosmic rays with the Earth's atmosphere, *Int. J. Modern Phys. A*, *20*(A11), 6802–6804.

- Dorman, L. (2010), *Solar Neutrons and Related Phenomena, Astrophysics and Space Science Library*, vol. 365, Springer, Dordrecht, Netherlands.
- Dorman, L. I., J. F. Valdés-Galicia, and I. V. Dorman (1999), Numerical simulation and analytical description of solar neutron transport in the Earth's atmosphere, *J. Geophys. Res.*, *104*, 22,417–22,426, doi:10.1029/1999JA900182.
- Dröge, W., D. Ruffolo, and B. Klecker (1996), Observation of electrons from the decay of solar flare neutrons, *Astrophys. J. Lett.*, *464*, L87, doi:10.1086/310093.
- Efimov, Y., and M. Terekhov (1988), Specific yield functions of neutron supermonitors for solar neutrons, *Geomagn. Aeron.*, *28*(5), 832–835.
- Efimov, Y. E. (1997), Registration of solar neutrons via neutron monitors, *Geomagn. Aeron.*, *37*, 498–500.
- Efimov, Y. E., G. E. Kocharov, and K. Kudela (1983), On the solar neutrons observation on high mountain neutron monitor, in *18th Int. Cosmic Ray Conference*, vol. 10, edited by P. V. Ramana Murthy, pp. 276–278, Tata Institute of Fundamental Research, Bombay, India.
- Engel, R., D. Heck, and T. Pierog (2011), Extensive air showers and hadronic interactions at high energies, *Annu. Rev. Nucl. Part. Sci.*, *61*, 467–489.
- Evenson, P., R. Kroeger, P. Meyer, and D. Reames (1990), Solar neutron decay proton observations in cycle 21, *Astrophys. J. Suppl.*, *73*, 273–277, doi:10.1086/191462.
- Gil, A., I. Usoskin, G. Kovaltsov, A. Mishev, C. Corti, and V. Bindi (2015), Can we properly model the neutron monitor count rate?, *J. Geophys. Res.*, *120*, 7172–7178, doi:10.1002/2015JA021654.
- Hatton, C. (1971), "The Neutron Monitor", *Progress in Elementary Particle and Cosmic-Ray Physics*, vol. 10, chap. 1, North Holland Publishing Co., Amsterdam.
- Hua, X.-M., and R. Lingenfelter (1987), Solar flare neutron production and the angular dependence of the capture gamma-ray emission, *Sol. Phys.*, *107*(2), 351–383.
- Hua, X.-M., B. Kozlovsky, R. Lingenfelter, R. Ramaty, and A. Stupp (2002), Angular and energy-dependent neutron emission from solar flare magnetic loops, *Astrophys. J. Suppl.*, *140*(2), 563–579.
- Kocharov, L., H. Debrunner, G. Kovaltsov, J. Lockwood, M. McConnell, P. Nieminen, G. Rank, J. Ryan, and V. Schoenfelder (1998), Deduced spectrum of interacting protons accelerated after the impulsive phase of the 15 June 1991 solar flare, *Astron. Astrophys.*, *340*, 257–264.
- Kocharov, L. G., J. W. Lee, H. Zirin, G. A. Kovaltsov, I. G. Usoskin, K. R. Pyle, M. A. Shea, and D. F. Smart (1994), Neutron and electromagnetic emissions during the 1990 May 24 solar flare, *Sol. Phys.*, *155*, 149–170, doi:10.1007/BF00670736.
- Kocharov, L. G., J. Torsti, R. Vainio, G. A. Kovaltsov, and I. G. Usoskin (1996), A joint analysis of high-energy neutrons and neutron-decay protons from a flare, *Sol. Phys.*, *169*, 181–207, doi:10.1007/BF00153840.
- Kuznetsov, S. N., V. G. Kurt, B. Y. Yushkov, K. Kudela, and V. I. Galkin (2011), Gamma-ray and high-energy-neutron measurements on CORONAS-F during the solar flare of 28 October 2003, *Sol. Phys.*, *268*, 175–193, doi:10.1007/s11207-010-9669-2.
- Matsubara, Y., et al. (2005), Search for solar neutrons associated with proton flares in solar cycle 23, in *Proceedings of 29th International Cosmic Ray Conference Pune*, vol. 1, pp. 17–20, Tata Institute of Fundamental Research, Mumbai.
- Mavromichalaki, H., et al. (2011), Applications and usage of the real-time neutron monitor database, *Adv. Space Res.*, *47*, 2210–2222.
- Mishev, A. L., I. G. Usoskin, and G. A. Kovaltsov (2013), Neutron monitor yield function: New improved computations, *J. Geophys. Res. Space Physics*, *118*, 2783–2788, doi:10.1002/jgra.50325.
- Muraki, Y., et al. (1995), Simultaneous observations of solar neutrons of June 6, 1991 at Mt. Haleakala and Mt. Norikura, in *24th Proc. International Cosmic Ray Conference*, vol. 4, pp. 175–178, Int. Union of Pure and Appl. Phys., Rome, Italy.
- Muraki, Y., et al. (2008), Detection of high-energy solar neutrons and protons by ground level detectors on April 15, 2001, *Astropart. Phys.*, *29*, 229–242, doi:10.1016/j.astropartphys.2007.12.007.
- Picone, J., A. Hedin, D. Drob, and A. Aikin (2002), NRLMSISE-00 empirical model of the atmosphere: Statistical comparisons and scientific issues, *J. Geophys. Res.*, *107*(A12), 1468, doi:10.1029/2002JA009430.
- Pyle, K. R., and J. A. Simpson (1991), Observation of a direct solar neutron event on 22 March 1991 with the Haleakala Hawaii, neutron monitor, in *22nd Proceedings of International Cosmic Ray Conference*, vol. 2, pp. 53–56, The Institute for Advanced Studies, Dublin, Ireland.
- Shea, M. A., D. F. Smart, and K. R. Pyle (1991), Direct solar neutrons detected by neutron monitors on 24 May 1990, *Geophys. Res. Lett.*, *18*, 1655–1658, doi:10.1029/91GL02001.
- Shibata, S. (1994), Propagation of solar neutrons through the atmosphere of the Earth, *J. Geophys. Res.*, *99*, 6651–6665, doi:10.1029/93JA03175.
- Smart, D. F., M. A. Shea, E. O. Flueckiger, H. Debrunner, and J. E. Humble (1990), Were solar neutrons observed by neutron monitors on 1984 April 25?, *Astrophys. J. Suppl.*, *73*, 269–272, doi:10.1086/191460.
- Stoker, P. H. (1987), Search for solar neutron recordings by the 18NM64 at Tsumeb during the 21ST solar cycle, in *Proceedings of the 20th International Cosmic Ray Conference*, vol. 3, pp. 98–100, Nuaka, Moscow.
- Struminsky, A., M. Matsuoka, and K. Takahashi (1994), Evidence of additional production of high-energy neutrons during the solar flare on 1991 June 4, *Astrophys. J.*, *429*, 400–405, doi:10.1086/174330.
- Usoskin, I., G. A. Kovaltsov, H. Kananen, and P. Tanskanen (1997), The world neutron monitor network as a tool for the study of solar neutrons, *Ann. Geophys.*, *15*, 375–386.
- Valdes-Galicia, J., Y. Muraki, K. Watanabe, Y. Matsubara, T. Sako, L. Gonzalez, O. Musalem, and A. Hurtado (2009), Solar neutron events as a tool to study particle acceleration at the Sun, *Adv. Space Res.*, *43*(4), 565–572.
- Vashenyuk, E., Y. Balabin, and P. Stoker (2007), Responses to solar cosmic rays of neutron monitors of a various design, *Adv. Space Res.*, *40*(3), 331–337.
- Vilmer, N., A. MacKinnon, and G. Hurford (2011), Properties of energetic ions in the solar atmosphere from γ -ray and neutron observations, *Space Sci. Rev.*, *159*(1–4), 167–224.
- Watanabe, K., et al. (2003), Solar neutron event in association with a large solar flare on 2000 November 24, *Astrophys. J.*, *592*, 590–596, doi:10.1086/375685.
- Watanabe, K., et al. (2007), Highly significant detection of solar neutrons on 2005 September 7, *Adv. Space Res.*, *39*, 1462–1466, doi:10.1016/j.asr.2006.10.021.
- Yu, X. X., H. Lu, G. T. Chen, X. Q. Li, J. K. Shi, and C. M. Tan (2015), Detection of solar neutron events and their theoretical approach, *New Astron.*, *39*, 25–35.
- Yue, A. T., M. S. Dewey, D. M. Gilliam, G. L. Greene, A. B. Laptev, J. S. Nico, W. M. Snow, and F. E. Wietfeldt (2013), Improved determination of the neutron lifetime, *Phys. Rev. Lett.*, *111*, 222501.
- Zusmanovich, A., and Y. F. Shwartsman (1987), Solar cosmic rays at the middle latitudes, in *Processes on the Surface and in the Interior of the Sun*, edited by G. Kocharov, Nauka, Moscow.